ADVANCED FUNCTIONAL MATERIALS
www.afm-journal.de
Materials Views
www.MaterialsViews.com

Polyhedral Oligosilsesquioxane-Modified Boron Nitride Nanotube Based Epoxy Nanocomposites: An Ideal Dielectric Material with High Thermal Conductivity

Xingyi Huang, Chunyi Zhi, Pingkai Jiang, Dmitri Golberg, Yoshio Bando, and Toshikatsu Tanaka*

Dielectric polymer composites with high thermal conductivity are very promising for microelectronic packaging and thermal management application in new energy systems such as solar cells and light emitting diodes (LEDs). However, a well-known paradox is that conventional composites with high thermal conductivity usually suffer from the high dielectric constant and high dielectric loss, while on the other hand, composite materials with excellent dielectric properties usually possess low thermal conductivity. In this work, an ideal dielectric thermally conductive epoxy nanocomposite is successfully fabricated using polyhedral oligosilsesquioxane (POSS) functionalized boron nitride nanotubes (BNNTs) as fillers. The nanocomposites with 30 wt% fraction of POSS modified BNNTs exhibit much lower dielectric constant, dielectric loss tangent, and coefficient of thermal expansion in comparison with the pure epoxy resin. As an example, below 100 Hz, the dielectric loss of the nanocomposites with 20 and 30 wt% BNNTs is reduced by one order of magnitude in comparison with the pure epoxy resin. Moreover, the nanocomposites show a dramatic thermal conductivity enhancement of 1360% in comparison with the pristine epoxy resin at a BNNT loading fraction of 30 wt%. The merits of the designed composites are suggested to originate from the excellent intrinsic properties of embedded BNNTs, effective surface modification by POSS molecules, and carefully developed composite preparation methods.

1. Introduction

The continuing miniaturization and increase of power density in electronic devices are setting higher and stricter requirements for performance, reliability, and processing techniques for advanced packaging materials.[1–8] Thermally conductive but electrically insulating materials become more and more important in the thermal management for energy systems such as solar power generation and light emitting diodes (LEDs).[9–11] Ideal materials for packaging and thermal management in microelectronic devices should have a low dielectric constant and dielectric loss, high thermal conductivity and easy processibility.[12] Although some ceramics possess high thermal conductivity and excellent electrical properties, it is difficult to process them into desirable final products. Polymers can offer excellent dielectric properties and remarkable processibility, but thermal conductivities for most of them are quite low (about 0.2 W m^{-1} K^{-1}).[12] Therefore, ceramic particle-filled polymer composites hold potential for electronic packaging applications by capitalizing on the ceramics' high thermal conductivity and prominent processibility of polymers. Recent studies have shown that by introducing ceramic particles with high thermal conductivity, such as aluminum nitride,[11] boron nitride,[13–15] silicon carbide,[16] and aluminum oxide[17] into polymers can result in a dramatic increase in the composite's thermal conductivity. However, a challenging problem faced is that adding ceramic particles with high thermal conductivity made of AlN and Al_2O_3 usually results in a serious deterioration of the dielectric properties of the fabricated composites, while on the other hand, ceramic particles with low dielectric constant and loss, such

Dr. X. Huang, Prof. P. Jiang
Department of Polymer Science and Engineering
Shanghai Key Lab of Electrical Insulation and Thermal Aging
Shanghai Jiao Tong University
Shanghai, 200240, China

Dr. C. Zhi
Department of Physics and Materials Science
City University of Hong Kong
Tat Chee Avenue, Kowloon, Hong Kong, China
E-mail: cy.zhi@cityu.edu.hk

Prof. D. Golberg, Prof. Y. Bando
International Center for Materials Nanoarchitectonics (MANA)
National Institute for Materials Science (NIMS)
Namiki 1-1, Tsukuba, Ibaraki 305-0044, Japan

Prof. T. Tanaka
IPS Research Cente
Waseda University
Kitakyushu, Fukuoka, Japan

DOI: 10.1002/adfm.201201824

as SiO_2 particles, cannot effectively improve the thermal conductivity of polymers.[16–22] Therefore, development of polymer composites with low dielectric constant and dielectric loss, as well as high thermal conductivity is of prime importance for various practical electronic packaging applications.

Boron nitride nanotubes (BNNTs) are prospective nanofillers for various applications due to their constant wide band gap (≈5.5 eV), superb thermal and antioxidation stability, high thermal conductivity and excellent mechanical properties.[20,23–34] Moreover, BNNTs were reported to possess a low dielectric constant. Keeping in mind that polyhedral oligosilsesquioxane (POSS) molecules may induce a local low dielectric constant area in composites and that BNNTs are surface modifiable,[35–38] it is expected that the POSS modified BNNTs are suitable for fabrication of polymer composites with a combination of optimal dielectric properties and high thermal conductivity.

In this work, POSS modified BNNTs are demonstrated to be very effective nanofillers for making dielectric epoxy composites with high thermal conductivity. A remarkably decreased dielectric constant and dielectric loss tangent were observed for such composites. Moreover, the materials possess a remarkably improved thermal conductivity and low coefficient of thermal expansion (CTE). This successfully solves the well-known problem that high thermal conductivity and low dielectric loss cannot be achieved simultaneously. The intrinsic dielectric properties and effective surface modification to BNNTs, as well as the composite fabrication procedures are suggested to be the key factors responsible.

2. Results and Discussion

BNNTs were grown using an optimized chemical vapor deposition using boron and metal oxide as reactants (BOCVD). The detailed procedure was reported elsewhere.[10,23,40,41] The as-grown BNNTs contain residual metal and metal oxide[42] with high electrical conductivity or high dielectric constant, which may ruin the dielectric properties of epoxy composites. Therefore, nitric acid (HNO_3) was used to remove these impurities before composite fabrication.[43] As shown in **Figure 1**, the purified BNNTs have a high aspect ratio and perfect tubular structure. The typical diameter is around 50 nm and the length can be up to tens of micrometers. These morphological characteristics make BNNTs desirable for composite applications. However, the fibrous structures of BNNTs create a challenge to fabricate uniform composites with high performance. First of all, it is very difficult to achieve the homogeneous dispersion of high fraction of BNNTs in a polymer matrix, especially for thermoset (e.g., epoxy resin) composites with high viscosity. The other drawback is precuring of epoxy resin during the solvent removal process. In the current work, these problems were effectively overcome by utilizing POSS molecules which functionalize BNNTs and adopting an original composite preparation method (see Figure S1 and S2 in the Supporting Information).

Figure 2 shows the general fabrication process of POSS functionalized BNNTs (BNNT-POSS). BNNTs were firstly oxidized by hydrogen peroxide, followed by connection of silane coupling agent and POSS molecules (see the Supporting Information for details).

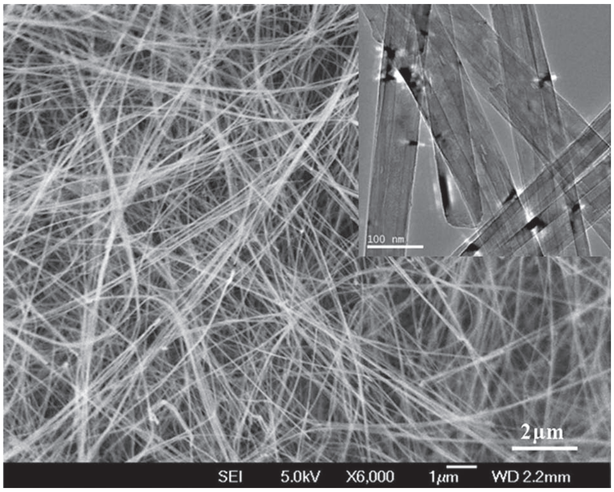

Figure 1. SEM image of BNNTs grown by BOCVD. Inset is a TEM image of the BNNTs.

Figure 3 depicts the typical TEM image and STEM electron energy loss spectroscopy (EELS) maps of BNNT-POSS. Some amorphous substance coated along the side wall of a nanotube is clearly observed. It should be noted that the intensity of carbon, oxygen, and silicon signals in EELS maps of BNNT-POSS was recorded solely on the nanotube surface. Fourier transform infrared spectrum (FTIR) confirmed the appearance of a peak at 1100 cm^{-1} (**Figure 4**) in the BNNT-POSS, which is a fingerprint of the presence of Si-O-Si bonds and absence of hydroxylated BNNTs (BNNT-OH) and silane modified BNNTs (BNNT-NH_2). These analyses confirm that POSS has been successfully grafted onto the surface of BNNTs. Thermogravimetric analysis (TGA) was further used to comparatively characterize the as-grown, purified and modified BNNTs. As shown in Figure 4, the total weight loss for BNNT-POSS is about 1.7%. In combination with weight loss data of pure POSS at the same experimental conditions (see Figure S3 in the Supporting Information), the total weight fraction of POSS grafted onto the surface of BNNTs was estimated to be about 2.45%.

Compared with pristine BNNTs, the modified BNNTs show much better dispersibility in various organic solvents, such as tetrahydrofuran (THF) (see Figure S4 in the Supporting information). Moreover, Raman studies reveal that the intrinsic crystalline properties of BNNTs were well preserved after modification (see Figure S5 in the Supporting information).[46] **Figure 5** illustrates the FE-SEM observations of the fractured surface of the BNNT-POSS based epoxy composites. It is evident that BNNTs are uniformly dispersed in the epoxy matrix. In addition, interface-debonding between BNNTs and the epoxy resin is not observed, suggesting the strong interfacial adhesion. Such uniform dispersion of BNNTs and strong interface are beneficial to the thermal conductivity enhancement of the nanocomposites, as discussed below.

Figure 6 presents the frequency-dependent dielectric properties of the epoxy/BNNT-POSS nanocomposites. It is surprising

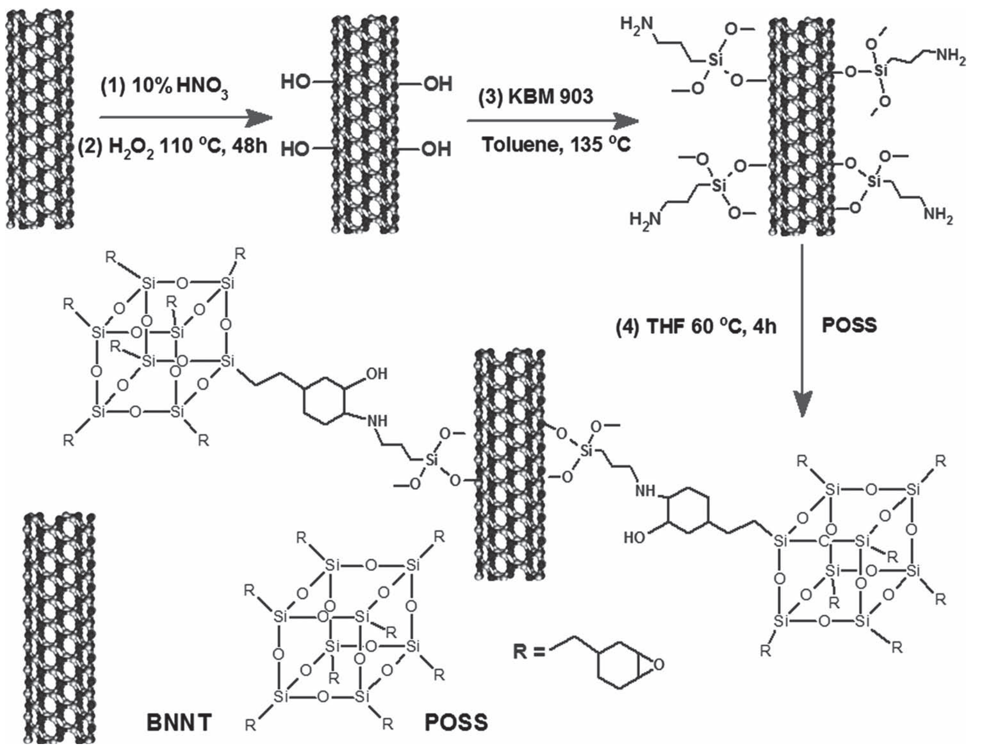

Figure 2. Schematic diagram illustrating a process of as-grown BNNTs transformation to POSS functionalized BNNTs. The detailed description is presented in the Supporting Information.

that both the dielectric constant and dielectric loss tangent of the nanocomposites are much lower than those of the epoxy resin over the whole frequency range. For instance, below 100 Hz, the dielectric loss of the nanocomposites with 20 and 30 wt% BNNTs is reduced by one order of magnitude in comparison with the pure epoxy resin. The dielectric constant of the epoxy resin is 4.1 at 100 Hz, whereas the nanocomposites have a value of about 3.6 irrespective of the BNNT content.

The introduction of inorganic fillers into an insulating matrix usually results in high dielectric loss.[16–22] Therefore, the observed dramatic decrease of the dielectric loss in epoxy/BNNTs nanocomposites is very unusual. It is even more surprising that the dielectric loss tangent of the nanocomposites decreases with an increase of BNNT content. **Table 1** summarizes previously reported dielectric property and thermal conductivity enhancement (TCE, defined as $\lambda_{\text{composites}}/\lambda_{\text{epoxy}}$) for epoxy composites with various fillers. The variations of dielectric constant ($\Delta\varepsilon$) is defined as $\Delta\varepsilon = \varepsilon_c/\varepsilon_p$, where ε_c and ε_p are the dielectric constant of the composites and polymer matrix, respectively. The variations of dielectric loss tangent ($\Delta\tan(\delta)$) is defined as $\Delta\tan\delta = \tan(\delta_c)/\tan\delta_p$, where $\tan(\delta_c)$ and $\tan(\delta_p)$ are the dielectric loss tangent of the composites and polymer matrix, respectively. As shown in Table 1, although the thermal conductivity is enhanced, the incorporation of SiC, Si_3N_4, AlN, BN, and Al_2O_3 in epoxy resins results in a much higher dielectric loss and higher dielectric constant in the composites. In addition, the dielectric loss and dielectric constant of epoxy composites usually increase with an increase in filler content. To the best of our knowledge, this is the first report on the observation of low dielectric constant and dielectric loss in epoxy composites which simultaneously exhibit high thermal conductivity.

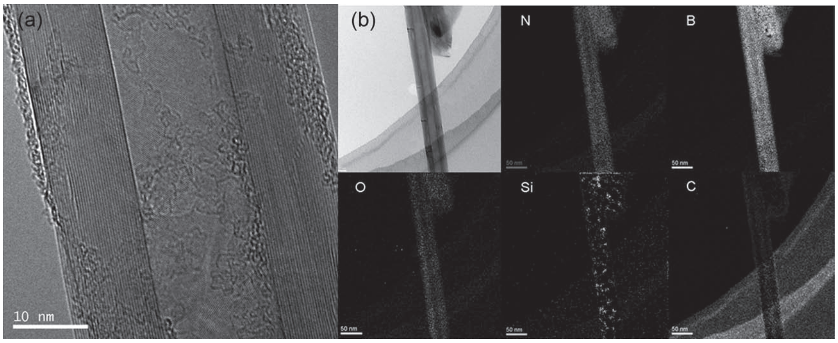

Figure 3. Typical a) TEM images and b) STEM electron energy loss spectroscopy maps of BNNT-POSS.

The dielectric loss tangent is closely associated with the electrical conductivity in the epoxy composites,[47–49] which is determined by a charge carrier density at the certain temperature. Therefore, the decreased dielectric loss tangent of epoxy/BNNT nanocomposites should be attributed to a reduction of the electrical conductivity, which is confirmed by the conductivity spectra of the composites (see Figure 6c). The terminal epoxy groups from the POSS grafted onto the BNNT surface can react with the curing agent (see Scheme 1 in the Supporting

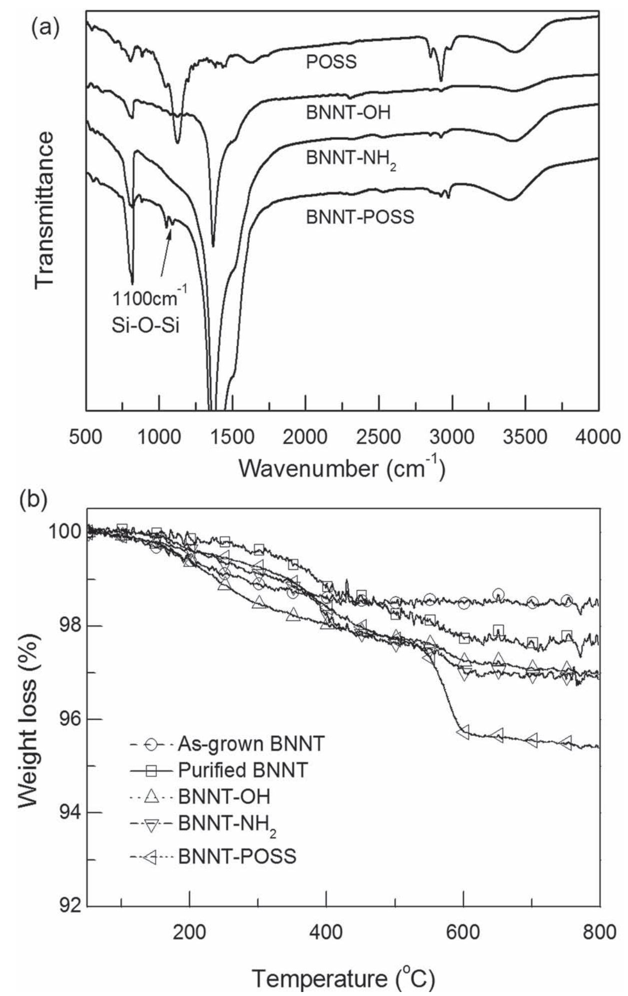

Figure 4. a) FTIR of POSS and modified BNNTs; b) TGA curves of various BNNTs. The purified BNNTs show less weight loss before 400 °C in comparison with the as-grown BNNTs, indicating existence of some thermally unstable substance in the as-grown BNNTs. The continuous weight reduction from 300 to 800 °C implies the existence of a few functional groups on the surface of BNNTs.[10,44], but the concentration and chemical activity of these functional groups are very low according to ref. [45]. BNNTs treated by H_2O_2 (BNNT-OH) shows the maximum weight loss before 300 °C, implying the successful introduction of -OH groups on the surface of BNNTs. The weight loss of BNNTs-NH_2 starting from 300 °C is attributed to the degradation of silane coupling agent.

information), forming a covalent interface between BNNTs and the polymer matrix. Moreover, the uniformly dispersed BNNTs may result in a large volume fraction of the interface between BNNTs and the polymer matrix. As a consequence, the mobility of the charge carriers is inhibited due to embedment of BNNTs. With a higher fraction of BNNTs, more interfaces are introduced, resulting in an effectively decreased dielectric loss. The low dielectric loss is very important for practical applications. Materials with high dielectric loss can produce much heat under electric field, which can finally ruin the performance, reliabilities and lifetime of electric devices and apparatus.

The low dielectric constant is also the key parameter for various applications such as interlayer dielectrics for the on-chip interconnection of ultralarge-scale integration devices, which is used to provide high operation speed, low dynamic power dissipation, and low cross-talk noise.[52] One of the possible reasons for lower dielectric constant obtained in the epoxy/BNNT composites is the relatively low intrinsic dielectric constant of hexagonal BNNTs (about 4).[9] Besides this factor, the other contribution may come from the restriction of bulk polarization in epoxy resin due to the immobility of polymer chains hindered by BNNTs.[47–49] The covalent bonds between polymer chains and BNNTs lead to the formation of a highly immobile epoxy nanolayer attached on the surface of BNNTs. Considering the nanometer-scale dimensions of BNNTs, it is estimated that a large portion of the immobilized epoxy-BNNT interface layer exists in the epoxy/BNNT nanocomposites.[48] The increase of glass transition temperature (see Figure S6 in the Supporting Information) of epoxy resin in the nanocomposites confirmed the strong interactions at the interface between BNNT-POSS and epoxy matrix. Epoxycyclohexyl POSS has short and rigid organic chains, which are effective in increasing the glass transition temperature in the interphase region.[53] POSS modification may be the other key factor for achieving low dielectric constant of the epoxy/BNNT nanocomposites, because POSS molecules can result in a low dielectric constant in the interface region.

The thermal conductivity of the epoxy/BNNT nanocomposites is shown in **Figure 7**. The room temperature thermal conductivity of the pure epoxy is about 0.2 W m^{-1} K^{-1}. The nanocomposites reveal dramatic enhancement of thermal conductivity in comparison with the pure epoxy. The highest measured room-temperature thermal conductivity is 2.77 W m^{-1} K^{-1} at 30.0 wt% BNNT fraction, which is 13.6 times higher than that of the pure epoxy resin. In combination with the TCE data summarized in Table 1, our results document that the measured thermal conductivity enhancement in our epoxy/BNNT nanocomposites is extremely high. It should be noted that the improvement of thermal conductivity in the present epoxy/BNNT nanocomposites is nonlinear: at a high fraction of BNNTs, a more effective improvement was observed. This implies that efficient thermal transfer pathways start to form at a high fraction of BNNTs due to tube-to-tube connections. It is believed that at a BNNT fraction of higher than 30 wt%, a more effective improvement is expected. Figure 7b presents the comparative thermal conductivity as a function of temperature for the epoxy and epoxy/BNNT nanocomposites. All the samples show a slight increase in thermal conductivity as the temperature increases from 25 to 150 °C.

One of the beneficial factors for the effective thermal conductivity improvement achieved is the homogeneous dispersion of BNNTs in the epoxy matrix as well as low defect density achieved via vacuum degassing and high-pressure curing. This guarantees high-quality uniform epoxy-BNNT composite samples, which may result in decreased phonon scattering. More importantly, the BNNTs used in our experiments were synthesized at 1500 °C. The high crystallinity and low defect density of BNNTs may lead to a high thermal conductivity of BNNTs and their composites. Taken CNTs as a reference,[54] we note that although well-crystallized and defect-free CNTs were reported

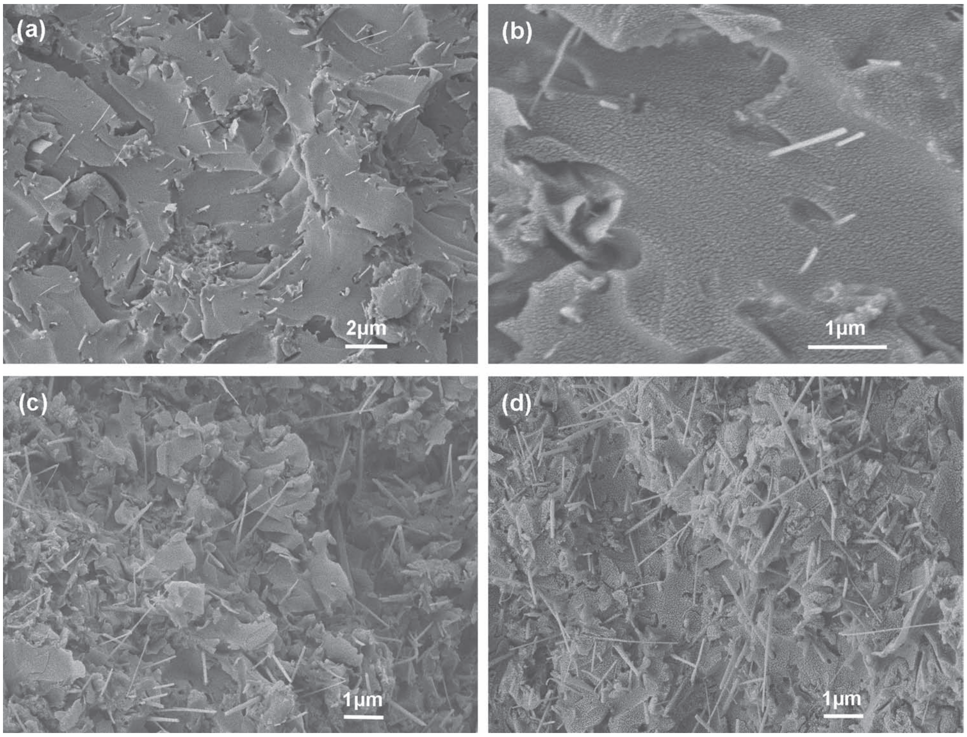

Figure 5. FE-SEM images of the epoxy/BNNT-POSS nanocomposites. a,b) 10 wt% BNNT-POSS, c) 20 wt% BNNT-POSS, d) 30 wt% BNNT-POSS. The tubes are seen as white rods.

to have thermal conductivity as high as 3000 W m^{-1} K^{-1}, the standard low temperature CVD-grown CNTs which exhibit entangled structures, numerous defects and low crystallinity (e.g., lattice defects, amorphous carbon, impurities, see Figure S7 in the Supporting Information), are prone to dramatically enhanced phonon scattering that reduces the thermal conductivity. For example, it was theoretically computed that thermal conductivity of CNTs decreases from 3500 to about 1250 W m^{-1} K^{-1} as the defect concentration increases from 0.05% to 0.25%.[55]

As an important parameter for thermally conductive composite materials, thermal boundary resistance was roughly calculated by the effective medium theory.[56] Fitting using this theory reveals that the thermal boundary resistance between BNNT-POSS and epoxy matrix is less than 1×10^{-9} m^2 K W^{-1}, which is relatively smaller in comparison with that of randomly dispersed CNTs in epoxy (10^{-8} to 10^{-7} m^2 K W^{-1}),[57] and comparable with that of aligned CNT epoxy composites.[59] This data indicates that an effective interfacial thermal transfer was indeed achieved in the BNNT-POSS epoxy composites.

As far as overall performances of thermally conductive dielectric materials are concerned, low coefficient of thermal expansion (CTE) is an important factor critical to the microelectronic packaging. A large difference in the CTEs between packaging materials and the components can result in serious internal stresses and thus poor reliability of a device. Reduction of the CTEs of packaging materials may minimize the CTE mismatch between the packaging materials and components. Thermal mechanical analysis (TMA) was used to investigate the thermal expansion behavior of the fabricated epoxy nanocomposites. **Figure 8** shows the thickness-normalized TMA curves, the slope of which reflects the CTEs. The CTE value of pure epoxy resin is 75×10^{-6} K^{-1}. A monotonic decrease in CTEs is observed in the nanocomposites as the content of BNNT-POSS increases. For the sample with 30 wt% fraction of BNNTs, the CTE is decreased by about 30%, which is even better than in case of AlN-epoxy composites.[59] It is believed that the covalent interactions between the epoxy matrix and POSS grafted on the BNNTs, and the physical confinement of epoxy are responsible for the effective CTEs reduction.

In order to show the superiority of POSS as a modifier of BNNT for the epoxy nanocomposites, a comparative investigation on the property of composites with 30 wt% BNNT-POSS, BNNT-NH_2 and BNNT-OH was performed. As shown in **Figure 9**, the dielectric constant and CTE values of the three composites show the order of BNNT-POSS < BNNT-NH_2 < BNNT-OH over the whole measurement frequency range, but the thermal conductivity and dielectric loss of the composites do not show a strict sequence. First, the composites with BNNT-POSS and BNNT-NH_2 show comparative thermal conductivities, and their values are higher than that of the composite with BNNT-OH. Second, although the dielectric loss of the composites with BNNT-NH_2 is higher than that of the composite containing BNNT-POSS over the whole measurement frequency range, the dielectric loss of the composite with BNNT-OH is higher than that of the composite containing BNNT-POSS only at the low frequency range, and both of the composites have the comparative dielectric loss at high frequency range. On

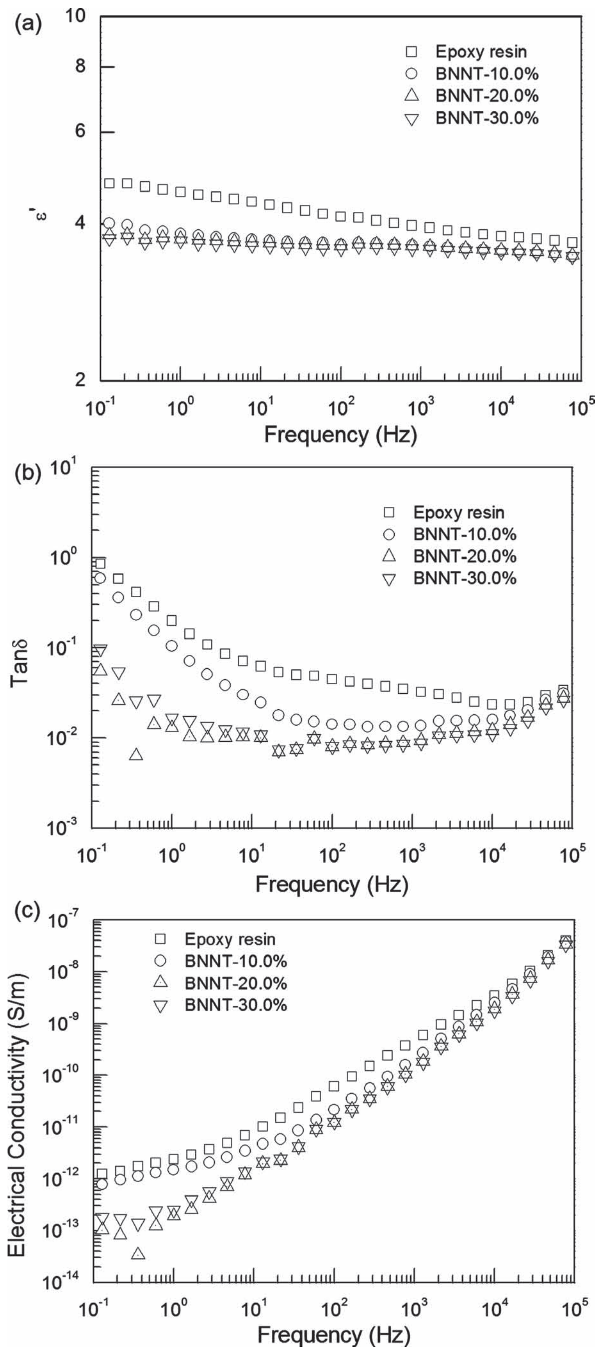

Figure 6. a) Frequency-dependent dielectric constant, b) dielectric loss tangent (tan(δ)), and c) electrical conductivity of the epoxy/BNNT-POSS nanocomposites.

the whole, however, the nanocomposites with BNNT-POSS are superior to those with BNNT-NH_2 and BNNT-OH. Namely, the BNNT-POSS based nanocomposites combine the lower dielectric constant, lower dielectric loss, high thermal conductivity and lower CTE. It seems that the unique geometry and multiple epoxide groups of POSS bring about the superior characteristics to the nanocomposites.

Table 1. Variations of dielectric constant ($\Delta\varepsilon$), dielectric loss tangent (Δtan(δ)) and thermal conductivity enhancement (TCE) in epoxy composites.

Filler	$\Delta\varepsilon$	$\Delta\tan\delta$	TCE	Fraction	Reference
SiC	187%	147%	<200%	13.8 vol%	[16,50]
Al_2O_3	137%	140%	138%	20 wt%	[51]
BN Powder	115%	220%	155%	20 wt%	[22]
BN Powder	122%	255%	190%	30 wt%	[22]
Si_3N_4	141%	483%	424%	20 vol%	[20]
Si_3N_4	151%	533%	545%	30 vol%`	[20]
AlN	112%	213%	180%	23.4 wt%	[18]
AlN	120%	265%	187%	27.4 wt%	[18]
BNNT	88%	18%	698%	20 wt%	This work
BNNT	87%	18%	1360%	30 wt%	This work

3. Conclusions

We successfully achieved the simultaneous properties of low dielectric constant, low dielectric loss, and high thermal conductivity in BNNT-POSS/epoxy composites, solving the well-known

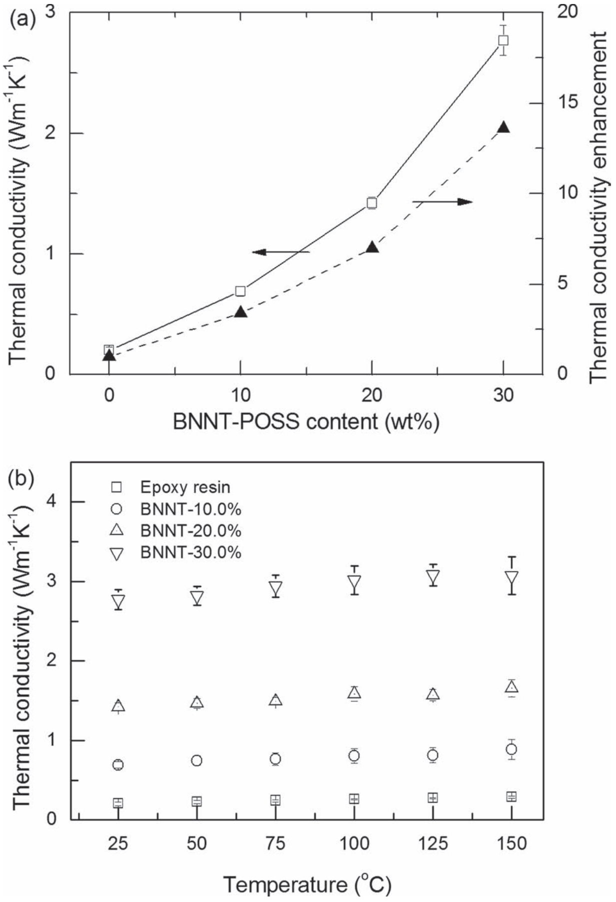

Figure 7. a) Thermal conductivity enhancement of epoxy/BNNT-POSS nanocomposites at 25 °C and b) temperature dependent thermal conductivity of epoxy/BNNT-POSS nanocomposites.

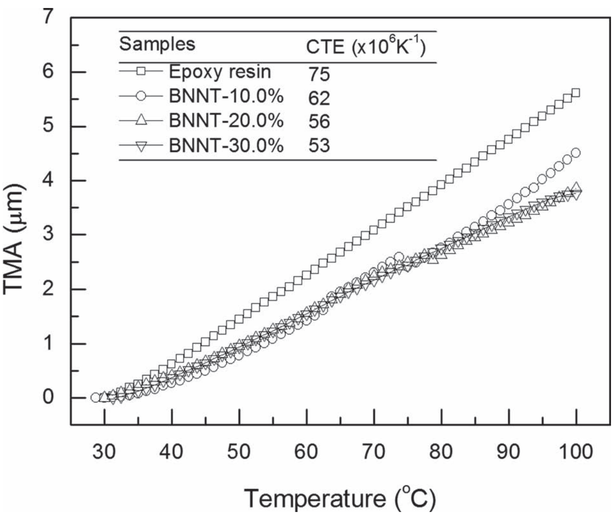

Figure 8. Thickness-normalized TMA for a pure epoxy resin and the epoxy/BNNT-POSS nanocomposites.

problem that thermally conductive polymer composites deteriorate the dielectric properties, and that the thermal conductivities of low-dielectric-loss polymer composites are usually low. In addition, the fabricated BNNTs-POSS epoxy composites possess effectively reduced coefficient of thermal expansion. These remarkable properties make the composites ideal dielectric materials for heat dissipation in electronic devices and equipments. The intrinsic low dielectric constant of embedded BNNTs and well-designed surface modification are suggested to be the key factors for achieving excellent dielectric properties. In addition, the high-quality BNNTs used and carefully-developed original composite fabrication techniques guarantee the uniform BNNT-POSS/epoxy composite samples with a low defect and void density, which result in effectively improved thermal conductivity and reduced CTEs. The excellent dielectric and thermal properties of the present nanocomposites may pave a way for comprehensive applications in electronic packaging and thermal management for energy systems, such as solar power generation devices and LEDs.

Supporting Information

Supporting Information is available from the Wiley Online Library or from the author.

Acknowledgements

X.Y.H. and P.K.J. gratefully acknowledge supports from the National Natural Science Foundation of China (Grant No. 51107081 and 51277117), the Research Fund for the Doctoral Program of Higher Education (Grant No. 20100073120038) and the Shanghai Leading Academic Discipline Project (Grant No. B202). This article was modified after online publication. The corresponding author's email address was corrected.

Received: June 26, 2012
Revised: August 31, 2012
Published online: November 6, 2012

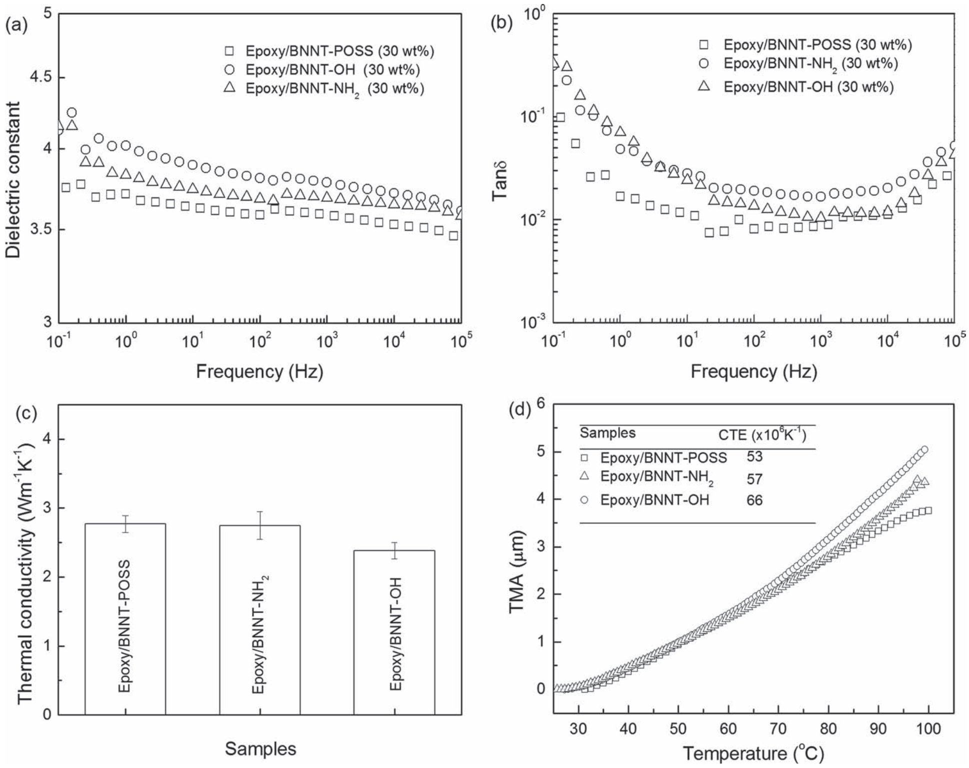

Figure 9. a) Frequency dependent dielectric constant, b) frequency dependent dielectric loss tangent (tan(δ)), c) thermal conductivity and d) thickness-normalized TMA for epoxy nanocomposites with BNNT-POSS, BNNT-NH$_2$, and BNNT-OH. All the nanocomposites contain 30 wt% BNNTs.

[1] a) J. K. Yang, Y. Yang, S. W. Waltermire, X. X. Wu, H. T. Zhang, T. Gutu, Y. F. Jiang, Y. F. Chen, A. A. Zinn, R. Prasher, T. T. Xu, D. Y. Li, *Nat. Nano.* **2012**, *7*, 91; b) M. D. Losego, M. E. Grady, N. R. Sottos, D. G. Cahill, P. V. Braun, *Nat. Mater.* **2012**, *11*, 502.

[2] a) K. M. F. Shahil, A. A. Balandin, *Nano Lett.* **2012**, *12*, 861; b) T. Luo, J. R. Lloyd, *Adv. Funct. Mater.* **2012**, *22*, 2495.

[3] a) P. E. Hopkins, M. Baraket, E. V. Barnat, T. E. Beechem, S. P. Kearney, J. C. Duda, J. T. Robinson, S. G. Walton, *Nano Lett.* **2012**, *12*, 590; b) H. Huang, C. H. Liu, Y. Wu, S. S. Fan, *Adv. Mater.* **2005**, *17*, 1652.

[4] a) L. M. Veca, M. J. Meziani, W. Wang, X. Wang, F. S. Lu, P. Y. Zhang, Y. Lin, R. Fee, J. W. Connell, Y. P. Sun, *Adv. Mater.* **2009**, *21*, 2088; b) A. P. Yu, P. Ramesh, M. E. Itkis, E. Bekyarova, R. C. Haddon, *J. Phys. Chem. C* **2007**, *111*, 7565.

[5] a) A. P. Yu, P. Ramesh, X. B. Sun, E. Bekyarova, M. E. Itkis, R. C. Haddon, *Adv. Mater.* **2008**, *20*, 4740; b) M. Bozlar, D. L. He, J. B. Bai, Y. Chalopin, N. Mingo, S. Volz, *Adv. Mater.* **2010**, *22*, 1654.

[6] a) C. Y. Zhi, Y. Bando, C. C. Tang, H. Kuwahara, D. Golberg, *Adv. Mater.* **2009**, *21*, 2889; b) X. P. Huang, G. Q. Liu, X. W. Wang, *Adv. Mater.* **2012**, *24*, 1482.

[7] J. Taha-Tijerina, T. N. Narayanan, G. Gao, M. Rohde, D. A. Tsentalovich, M. Pasquali, P. M. Ajayan, *ACS Nano* **2012**, *6*, 1214.

[8] Q. Liang, X. Yao, W. Wang, Y. Liu, C. P. Wong, *ACS Nano* **2011**, *5*, 2392.

[9] E. S. Lee, S. M. Lee, D. J. Shanefield, W. R. Cannon, *J. Am. Chem. Soc.* **2008**, *91*, 1169.

[10] C. Y. Zhi, Y. Bando, C. C. Tang, Q. Huang, D. Golberg, *J. Mater. Chem.* **2008**, *18*, 3900.

[11] Y. S. Xu, D. D. L. Chung, *Compos. Interfaces* **2000**, *7*, 243.

[12] a) X. Y. Huang, P. K. Jiang, T. Tanaka, *IEEE Electr. Insul. M.* **2011**, *27*, 8; b) X. Y. Huang, T. Iizuka, P. K. Jiang, Y. Ohki, T. Tanaka, *J. Phys. Chem. C* **2012**, *116*, 13629.

[13] C. Y. Zhi, Y. Bando, T. Terao, C. C. Tang, H. Kuwahara, D. Golberg, *Adv. Funct. Mater.* **2009**, *19*, 1857.

[14] W. L. Song, P. Wang, L. Cao, A. Anderson, M. J. Meziani, A. J. Farr, Y. P. Sun, *Angew. Chem. Int. Ed.* **2012**, *51*, 6498.

[15] Z. B. Wang, T. Iizuka, M. Kozako, Y. Ohki, T. Tanaka, *IEEE Trans. Dielectr. Electr. Insul.* **2011**, *18*, 1963.

[16] T. L. Zhou, X. Wang, M. Y. Gu, D. S. Xiong, *Polym. J.* **2009**, *41*, 51.

[17] M. Kozako, Y. Okazaki, M. Hikita, T. Tanaka, in Proc. IEEE Int. Conf. Solid Dielectrics, Potsdam, **2010**, p. 1.

[18] W. Y. Peng, X. Y. Huang, J. H. Yu, P. K. Jiang, W. H. Liu, *Composites, Part A* **2010**, *41*, 1201.

[19] X. Y. Huang, L. Y. Xie, P. K. Jiang, G. L. Wang, F. Liu, *J. Phys. D: Appl. Phys.* **2009**, *42*, 245407.

[20] M. Terrones, J. M. Romo-Herrera, E. Cruz-Silva, F. Lopez-Urias, E. Munoz-Sandoval, J. J. Velazquez-Salazar, H. Terrones, Y. Bando, D. Golberg, *Mater. Today* **2007**, *10*, 30.

[21] Y. P. Zheng, J. X. Zhang, Q. Li, W. W. Chen, X. L. Zhang, *Polym. Plast. Technol. Eng.* **2009**, *48*, 384.

[22] J. Gu, Q. Zhang, J. Dang, C. Xie, *Polym. Adv. Technol.* **2012**, *23*, 1025.

[23] C. Y. Zhi, Y. Bando, C. C. Tang, D. Golberg, *Mater. Sci. Eng., R.* **2010**, *70*, 92.

[24] J. Yu, Y. Chen, R. Wuhrer, Z. W. Liu, S. P. Ringer, *Chem. Mater.* **2005**, *17*, 5172.

[25] Y. Chen, J. D. Fitz Gerald, J. S. Williams, S. Bulcock, *Chem. Phys. Lett.* **1999**, *299*, 260.

[26] W. Q. Han, W. Mickelson, J. Cumings, A. Zettl, *Appl. Phys. Lett.* **2002**, *81*, 1110.

[27] C. H. Lee, J. Drelich, Y. K. Yap, *Langmuir* **2009**, *25*, 4853.

[28] C. H. Lee, J. S. Wang, V. K. Kayatsha, J. Y. Huang, Y. K. Yap, *Nanotechnology* **2008**, *19*, 455605.

[29] P. Jaffrennou, J. Barjon, T. Schmid, L. Museur, A. Kanaev, J. S. Lauret, C. Y. Zhi, C. Tang, Y. Bando, D. Golberg, B. Attal-Tretout, F. Ducastelle, A. Loiseau, *Phys. Rev. B* **2008**, *77*, 235422.

[30] C. W. Chang, A. M. Fennimore, A. Afanasiev, D. Okawa, T. Ikuno, H. Garcia, D. Y. Li, A. Majumdar, A. Zettl, *Phys. Rev. Lett.* **2006**, *97*, 085901.

[31] A. Zettl, C. W. Chang, G. Begtrup, *Phys. Status Solidi B* **2007**, *244*, 4181.

[32] D. Golberg, X. D. Bai, M. Mitome, C. C. Tang, C. Y. Zhi, Y. Bando, *Acta Mater.* **2007**, *55*, 1293.

[33] X. D. Bai, D. Golberg, Y. Bando, C. Y. Zhi, C. C. Tang, M. Mitome, K. Kurashima, *Nano Lett.* **2007**, *7*, 632.

[34] W. Q. Han, H. G. Yu, C. Zhi, J. Wang, Z. Liu, T. Sekiguchi, Y. Bando, *Nano Lett.* **2008**, *8*, 491.

[35] A. Gomathi, S. J. Hoseini, C. N. R. Rao, *J. Mater. Chem.* **2009**, *19*, 988.

[36] S. Pal, S. R. C. Vivekchand, A. Govindaraj, C. N. R. Rao, *J. Mater. Chem.* **2007**, *17*, 450.

[37] W. L. Wang, Y. Bando, C. Y. Zhi, W. Y. Fu, E. G. Wang, D. Golberg, *J. Am. Chem. Soc.* **2008**, *130*, 8144.

[38] H. B. Zeng, C. Y. Zhi, Z. H. Zhang, X. L. Wei, X. B. Wang, W. L. Guo, Y. Bando, D. Golberg, *Nano Lett.* **2010**, *10*, 5049.

[39] C. Y. Zhi, T. Terao, Y. Bando, C. C. Tang, D. Golberg, *Pure Appl. Chem.* **2010**, *82*, 2175.

[40] C. Y. Zhi, Y. Bando, C. C. Tan, D. Golberg, *Solid State Commun.* **2005**, *135*, 67.

[41] C. Tang, Y. Bando, T. Sato, K. Kurashima, *Chem. Commun.* **2002**, 1290.

[42] C. Y. Zhi, Y. Bando, C. C. Tang, D. Golberg, *Solid State Commun.* **2011**, *151*, 183.

[43] C. Y. Zhi, Y. Bando, C. C. Tang, S. Honda, H. Kuwahara, D. Golberg, *J. Mater. Res.* **2006**, *21*, 2794.

[44] C. Y. Zhi, Y. Bando, C. C. Tang, H. Kuwahara, D. Golberg, *J. Phys. Chem. C* **2007**, *111*, 1230.

[45] C. Y. Zhi, Y. Bando, T. Terao, C. C. Tang, H. Kuwahara, D. Golberg, *Chem. Asian J.* **2009**, *4*, 1536.

[46] R. Arenal, A. C. Ferrari, S. Reich, L. Wirtz, J. Y. Mevellec, S. Lefrant, A. Rubio, A. Loiseau, *Nano Lett.* **2006**, *6*, 1812.

[47] T. Tanaka, *IEEE Trans. Dielectr. Electr. Insul.* **2005**, *12*, 914.

[48] T. Tanaka, M. Kozako, N. Fuse, Y. Ohki, *IEEE Trans. Dielectr. Electr. Insul.* **2005**, *12*, 669.

[49] T. Tanaka, G. C. Montanari, R. Mulhaupt, *IEEE Trans. Dielectr. Electr. Insul.* **2004**, *11*, 763.

[50] T. L. Zhou, X. Wang, X. H. Liu, D. S. Xiong, *Carbon* **2010**, *48*, 1171.

[51] J. H. Yu, R. M. Huo, C. Wu, X. F. Wu, G. L. Wang, P. K. Jiang, *Macromol. Res.* **2012**, *28*, 816.

[52] M. R. Baklanov, K. Maex, *Philos. Trans. R. Soc., A* **2006**, *364*, 201.

[53] Z. Y. Lin, S. Lau, K. S. Moon, C. P. Wong, in IEEE 62nd Electronic Components and Technology Conference (ECTC), San Diego, **2012**, p. 1599.

[54] Z. D. Han, A. Fina, *Prog. Polym. Sci.* **2011**, *36*, 914.

[55] J. W. Che, T. Cagin, W. A. Goddard, *Nanotechnology* **2000**, *11*, 65.

[56] C. W. Nan, G. Liu, Y. H. Lin, M. Li, *Appl. Phys. Lett.* **2004**, *85*, 3549.

[57] T. C. Clancy, S. J. V. Frankland, J. A. Hinkley, T. S. Gates, *Int. J. Therm. Sci.* **2010**, *49*, 1555.

[58] A. M. Marconnett, N. Yamamoto, M. A. Panzer, B. L. Wardle, K. E. Goodson, *ACS Nano* **2011**, *5*, 4818.

[59] K. C. Yung, B. L. Zhu, J. Wu, T. M. Yue, C. S. Xie, *J. Polym. Sci., Part B: Polym. Phys.* **2007**, *45*, 1662.